Investigation of Gene Expressions of Myeloma Cells in the Bone Marrow of Multiple Myeloma Patients by Transcriptome Analysis

Melda Sarıman[1], Neslihan Abacı[1], Sema Sırma Ekmekçi[1], Aris Çakiris[1], Ferda Perçin Paçal[1], Duran Üstek[1], Mesut Ayer[2], Mustafa Nuri Yenerel[3], Sevgi Beşışık[4], Kıvanç Çefle[5], Şükrü Palandüz[5], Şükrü Öztürk[5]

[1]Department of Genetics, İstanbul University, Aziz Sancar Experimental Medical Research Institute, İstanbul, Turkey
[2]Clinic of Hematology, İstanbul Haseki Training and Research Hospital, İstanbul, Turkey
[3]Department of Hematology, İstanbul Universiy İstanbul School of Medicine, İstanbul, Turkey
[4]Department of Internal Medicine, İstanbul Universiy İstanbul School of Medicine, İstanbul, Turkey
[5]Department of Internal Medicine, Division of Medical Genetics, İstanbul Universiy İstanbul School of Medicine, İstanbul, Turkey

Background: Multiple myeloma is a plasma cell dyscrasia characterized by transformation of B cells into malignant cells. Although there are data regarding the molecular pathology of multiple myeloma, the molecular mechanisms of the disease have not been fully elucidated.

Aims: To investigate the gene expression profiles in bone marrow myeloma cells via RNA-sequencing technology.

Study Design: Cell study.

Methods: Myeloma cells from four patients with untreated multiple myeloma and B cells from the bone marrow of four healthy donors were sorted using a FACSAria II flow cytometer. The patient pool of myeloma cells and the control pool of B cells were the two comparative groups. A transcriptome analysis was performed and the results were analyzed using bioinformatics tools.

Results: In total, 18.806 transcripts (94.4%) were detected in the pooled multiple myeloma patient cells. A total of 992 regions were detected as new exon candidates or alternative splicing regions. In addition, 490 mutations (deletions or insertions), 1.397 single nucleotide variations, 415 fusion transcripts, 132 frameshift mutations, and 983 fusions, which were reported before in the National Center for Biotechnology Information, were detected with unknown functions in patients. A total of 35.268 transcripts were obtained (71%) (25.355 transcripts were defined previously) in the control pool. In this preliminary study, the first 50 genes were analyzed with the MSigDB, Enrichr, and Panther gene set enrichment analysis programs. The molecular functions, cellular components, pathways, and biological processes of the genes were obtained and statistical values were determined using bioinformatics tools and are presented as a supplemental file.

Conclusion: *EEF1G*, *ITM2C*, *FTL*, *CLPTM1L*, and *CYBA* are identified as possible candidate genes associated with myelomagenesis.

Keywords: Flow cytometry, gene expresion, multiple myeloma, plasma cell dyscrasias, transcriptome analyses

Multiple myeloma (MM) is a cancer of plasma cells in which abnormal types of immunoglobulins are produced that can be measured in blood and urine (1). MM is a clonal B cell malignancy characterized by a clinical pentad in the bone marrow (2). According to the National Cancer Institute Surveillance, Epidemiology, and Results Program in 2017, 30,280 new cases of MM were diagnosed, and 12,590 deaths occurred in the United States (3).

The etiology of MM depends on many factors, such as the environment, chemical agents, viruses, and genetic factors (4). MM is caused by several molecular mechanisms, such as activation of oncogenes, genomic instability, and chromosome abnormalities

(5). Accumulated plasma cells in the bone marrow of patients with MM are identified by surface membrane antigens, such as CD38, CD138, CD56, CD117, and CD33. Although most myeloma cells typically express CD38(+), CD138(+), CD56(+), and CD19(-), these cells may indicate genetic heterogeneity (6). Next generation sequencing is evolving rapidly, and RNA-seq has become a widely used tool for understanding the molecular mechanisms of human cancers. The transcriptome is the complete set of transcripts in a cell that allows for the identification of exons and alternative splicing/ isoforms and novel RNAs. Massive parallel sequencing platforms are used to measure the differential expression of transcripts (7).

Cite this article as:
Sarıman M, Abacı N, Ekmekçi SS, Çakiris A, Perçin Paçal F, Üstek D et al. Investigation of Gene Expressions of Myeloma Cells in the Bone Marrow of Multiple Myeloma Patients by Transcriptome Analysis. Balkan Med J 2019;36:23-31

In the present study, we provide comprehensive insight into the transcriptomes of patients with MM and healthy donors. Many of the genes were determined in transcriptome profiles of pooled myeloma cells and were determined to play a role in MM pathogenesis via intracellular pathways, gene expression patterns, biological functions, and protein-protein interactions using *in silico* tools. Our transcriptomic profile obtained data to evaluate differential expression of all transcripts, alternative new splicing variants, mutations, and fusion genes. These results will contribute to the understanding of myeloma pathogenesis and provide valuable information for prognostication and new therapies.

MATERIALS AND METHODS

Sample collection

This study was approved (2010/108-28) by the Ethics Committee of İstanbul University Faculty of Medicine. Written informed consent Helsinki Declaration and ethics committee documents was obtained from all patients and healthy donors. We performed RNA-seq using the Ion Torrent Personal Genome Machine (PGM) platform to compare the transcriptome profiles of four newly diagnosed patients with untreated MM and four healthy donors. Bone marrow was aspirated from the hip bones of all patients and donors. The bone marrow samples were subjected to Ficoll gradient centrifugation (1.077 g/mL Ficoll), and the mononuclear cells were collected. The viability and absolute cell counts were determined by the Vi-CELL™ XR Cell Counter (Beckman Coulter, Brea, CA, USA).

Fluorescence-activated cell sorting

Myeloma cells (CD38$^+$, CD138$^+$, CD19$^-$, and CD56$^+$) and healthy B cells (CD38$^+$, CD138$^+$, CD19$^+$, and CD56$^-$) were selected from bone marrow mononuclear cells using a gating strategy by simultaneously specifying cell surface markers, and by determining forward and side light scattering characteristics on the FACSAria II Cell Sorter (Becton Dickinson, San Jose, CA, USA) (Figures 1, 2). The antibodies used for activating fluorescence and cell sorting were CD138/SYNDECAN-1 (cat: 347216) allophycocyanin, CD38 (cat: 340909) fluorescein isothiocyanate, CD19 (cat: 345777) phycoerythrin, CD56 (cat: 557747), and phycoerythrin cyanin (Becton Dickinson). The cells were passed through a 100 μm nozzle tip at a speed of approximately 50,000 events per sec. The images were taken and the analysis was performed using FACS Diva Software 6.1.2. The sorted cells were frozen for RNA isolation.

RNA isolation

RNA was extracted from the sorted cells using the PureLink RNA Microkit (cat: 12183_016; Invitrogen, Carlsbad, CA, USA). Before proceeding to rRNA depletion, the quantity and quality of total RNA was evaluated using the RNA 6000 Pico kit on the Agilent 2100 Bioanalyzer (Agilent Technologies, Anaheim, CA, USA). After checking the quantity and quality of the RNA, we pooled the RNA samples from the four untreated MM patients and four healthy donors. The workflow of the study is summarized in Table 1.

rRNA depletion

rRNA depletion was performed using the Eukaryotic Ribominus kit (cat no: A10837_2/A10837_08; Invitrogen). The quantity and
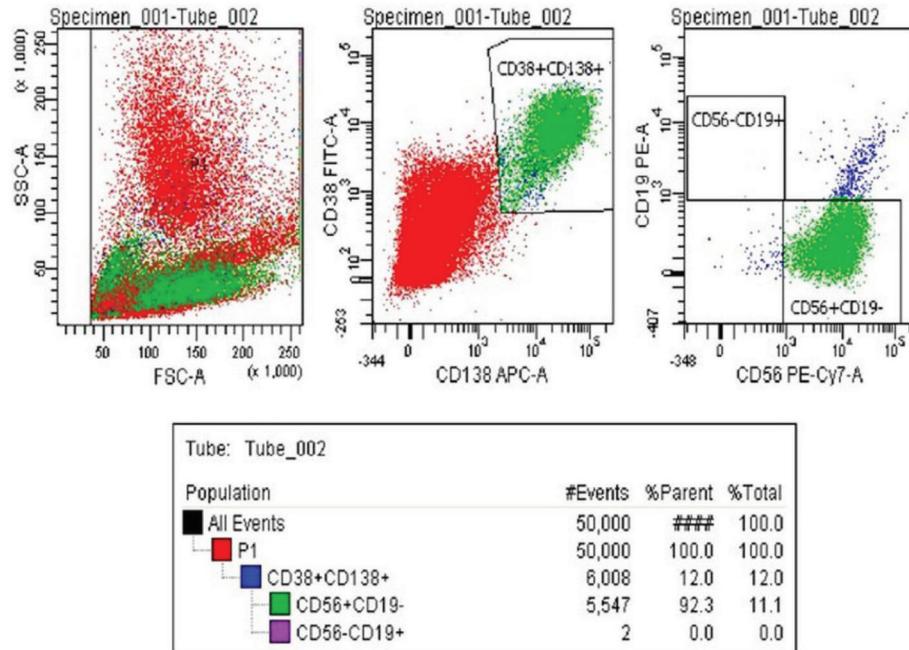
FIG. 1. Flow cytometry results of malignant B cells from bone marrow of a patient with Multiple myeloma. First, myeloma cells were gated by using specific cell surface markers that were CD138$^+$ and CD38$^+$ by determining forward and side light scattering characteristics on the FACSAria II Cell Sorter (Becton Dickinson, San Jose, CA, USA). Then sorted malignant Multiple myeloma cells using with cell sorting by the cell surface markers CD56$^+$, CD19$^-$ according to the FACSAria II Cell Sorter.

quality of the mRNA was evaluated using the RNA 6000 Pico kit on Agilent 2100 Bioanalyzer.

Library preparation and RNA sequencing

The RNA-sequencing libraries were prepared from the pooled RNA of the patients and healthy donors. The libraries were constructed using the Ion Total RNA-seq V2 kit protocol for transcriptome profiling of low-input RNA samples (April 2011). The quality of the libraries was validated using the Agilent High Sensitivity DNA kit on the Agilent 2100 Bioanalyzer (Figure 3). The final library concentrations were calculated after validating the libraries, using

the Ion PGM™ 200 Xpress Template kit (cat no: 4474280). Each library was amplified by Emulsion polymerase chain reaction of ion sphere particles (ISPs). These ISPs were recovered from the emulsion. The templated ISPs and unbound ISPs were determined by fluorometric assay on Qubit® 2.0.

The Ion PGM™ system was cleaned and initialized before sequencing. Sequencing was accomplished using the Ion PGM™ 200 Sequencing v2 kit (cat: 4474004; Life Technologies, Carlsbad, CA, USA) according to the manufacturer's instructions. Pooled samples were sequenced with a semiconductor-based sequencing
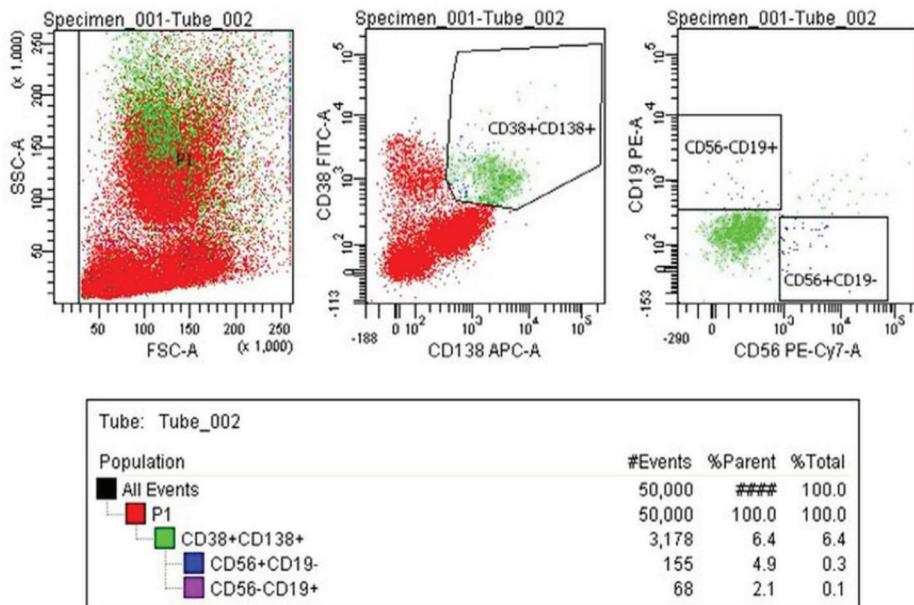

FIG. 2. Bone marrow B cell flow cytometry results from a healthy donor. First, B cells were gated by using specific cell surface markers that were CD138$^+$ and CD38$^+$ by determining forward and side light scattering characteristics on the FACSAria II Cell Sorter (Becton Dickinson, San Jose, CA, USA). Then sorted B cells using with cell sorting by the cell surface markers CD56$^+$, CD19$^+$ according to the FACSAria II Cell Sorter.
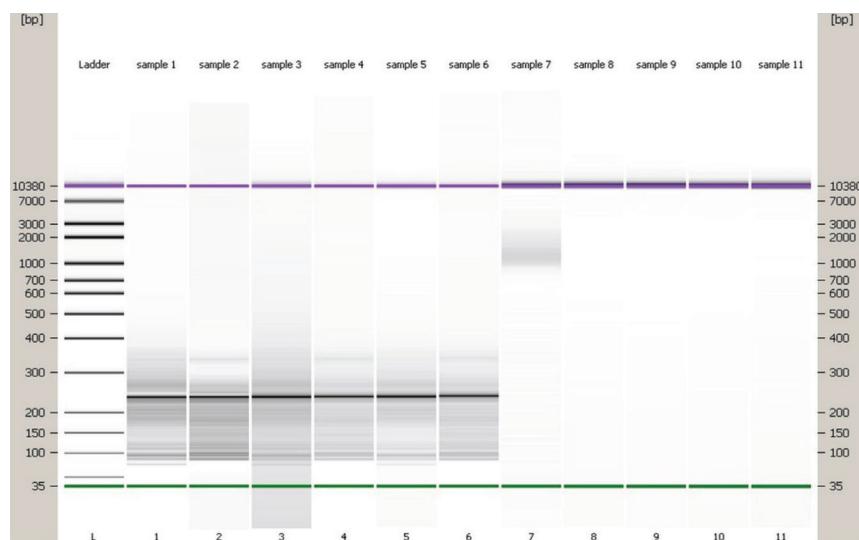
FIG. 3. In Agilent Bioanalyzer gel-like image of cDNA. This image shows produced cDNA samples quality controls. After library construction for the quality of the libraries was validated using the Agilent High Sensitivity DNA kit on the Agilent 2100 Bioanalyzer. DNA ladder (L), Lanes 1-3-5 (control cDNA library), the lanes 3-5 are ten-fold diluted sample 1. Lanels 2-4-6 (Multiple myeloma cDNA library). The lanes 4-6 are ten- fold diluted sample 2. Lane 7 (negative). Green lines indicate the low weight (35 base pairs) DNA ladder, Purple lines the high weight (10380 base pairs) DNA ladder.

system using the Ion 318™ Chip (lots: P30518.1, AA0150428, and AA0150429; Life Technologies).
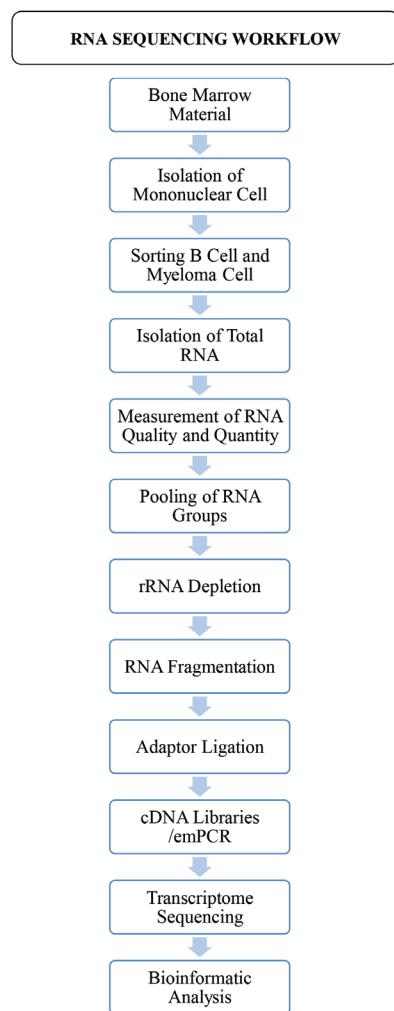
RNA-sequencing analysis

The pooled RNA from the patients with MM and that from the controls was subjected to massively parallel cDNA sequencing at İstanbul University Whole Genome Sequencing Laboratory Aziz Sancar Institute of Experimental Medicine. The sequencing data were analyzed with the PSSC Labs Big Data Server (Lake Forest, CA, USA). The quality of the raw sequencing data was checked and the data were preprocessed according to two criteria: adaptors and low quality sequences (readings with ambiguous N's) were removed, and data with a quality score (Qscore) <30 was trimmed.

Bioinformatics analysis

The trimmed sequencing reads were aligned to the UCSC human reference genome (build GRCh37/hg19) using TopHat v2.0.6, which incorporates Bowtie v0.12.8 software to build the alignment. The expression level for each transcript was normalized to the reads per kilobase of the exon model per million mapped reads (RPKM) (8). Cufflinks v2.0.2 was used to operate the original

TABLE 1. RNA-sequencing workflowcells

RNA SEQUENCING WORKFLOW

- Bone Marrow Material
- Isolation of Mononuclear Cell
- Sorting B Cell and Myeloma Cell
- Isolation of Total RNA
- Measurement of RNA Quality and Quantity
- Pooling of RNA Groups
- rRNA Depletion
- RNA Fragmentation
- Adaptor Ligation
- cDNA Libraries /emPCR
- Transcriptome Sequencing
- Bioinformatic Analysis

alignment file generated by tophat and the gene transfer format file for genome annotation to determine the difference between the expressed genes. The first 50 genes from the pooled MM RNA that were highly differentially expressed were analyzed using the Gene Set Enrichment Analysis (GSEA) program (Figure 4) and also demonstrated protein interactions.

RESULTS

The cDNA libraries from the patients with MM and the control group were subjected to massively parallel transcriptome sequencing. Of the 18,806 total transcripts obtained by the transcriptome analysis, 17,760 were reported previously in pooled patients with MM. These transcripts were used in the downstream analysis.

In total, 992 regions were detected and were candidates for new exons or alternative splicing regions. In addition, 490 deletions or insertions and 1.397 single nucleotide variations were detected; 415 fusion transcripts were defined. A total of 983 fusions, which were reported before in National Center for Biotechnology Information, were detected with unknown functions. In total, 132 frame shift mutations were identified in pooled patients with MM; 35,268 transcripts were obtained (71%) (25,355 transcripts were defined previously) in the control pool. Qscore values of about 35% on average for each chromosome were calculated. We measured the transcript values and identified the differentially expressed genes between the two groups using Cuffdiff/Cuflink. In total, we detected 12,453 expressed genes by calculating reads per kilobase million (RPKM) values and analyzed the data from the first 50 highly expressed selected genes in the pooled MM cells (Table 2) and compared the expression levels with the controls (Table 3). The eukaryotic elongation factor 2 (*EEF2*) gene was the most significantly expressed gene among the MM and normal cells according to our RPKM results. Our analysis included the majority of annotated human genes. The analysis of the whole transcriptome data revealed different expression levels of several genes, such as *JAK1*, *JAK2*, *JAK3*, *RAF*, *IL6R*, *NCAM (CD56)*, *WHSC1*, *MCL1*, *BCL2,* and *IGF1*, which showed myeloma pathogenesis as reported previously. These 50 genes were subjected to the GSEA using MSigDB. As a result, 11 of these genes had increased expression in plasma cells from patients with MM that significantly overlapped between *EEF1A1*, *UBC*, *UBB*, *CALR*, *CXCR4*, *JUND*, *FOS*, *PIM2*, *JUN*, *GAPDH*, and *HSP90B1* and were previously reported as upregulated in the Munshi_multiple _myeloma data set (Figure 4). The biological functions, molecular processes, and pathways of these genes were determined using the online tool Panther-GO (Figures 5-7). These genes were also analyzed by the String v9.0 program to demonstrate protein-protein interactions (Figure 8). We performed the bioinformatics calculations using the Enrichr GSEA program. Computational bioinformatics was used to explore the deep relationships between the genes in the annotated gene sets and between other data sets. We investigated and visualized the overlap between our data sets within the Enrichr program to compare with other web-server tools and resources that serve gene set libraries. The molecular functions, cellular components, pathways, and biological processes are presented as a supplemental file.
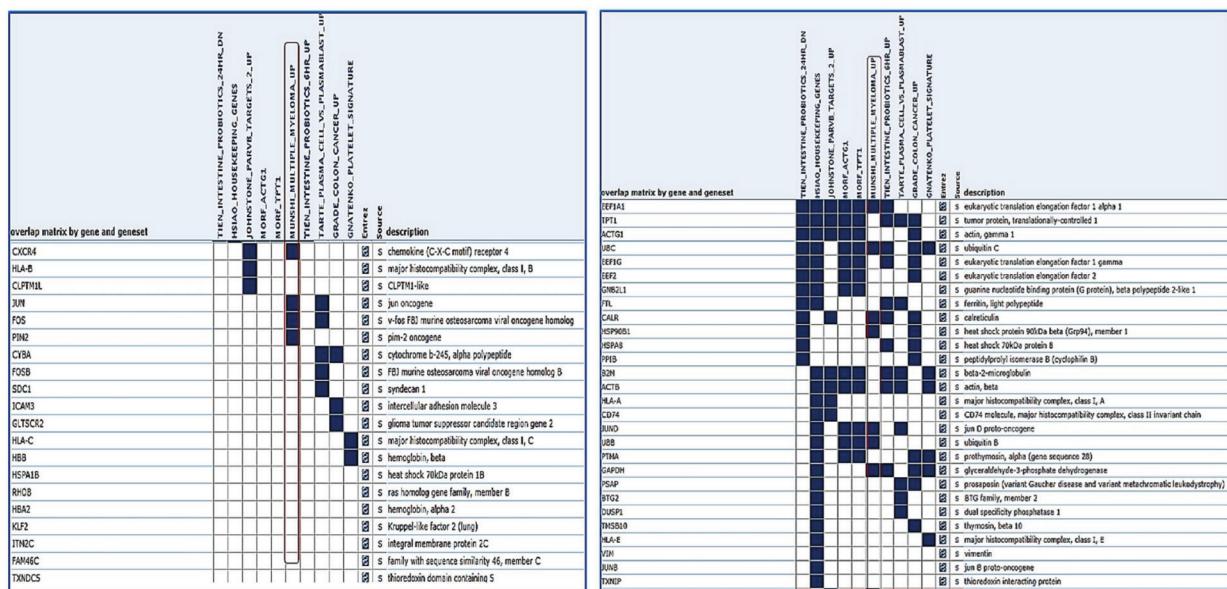
FIG. 4. The first 50 highly expressed selected genes in the pooled Multiple myeloma cells results of the Gene Set Enrichment Analysis-MSigDB program. Summary figures displayed enriched gene sets with three major columns: gene names, the images of overlapping between gene and gene sets, descriptions of gene names. These 50 genes to compare with other gene set libraries subjected to the Gene Set Enrichment Analysis using MSigDB. Shown in the figure, 11 of these genes had increased expression in myeloma cells that significantly overlapped between *EEF1A1*, *UBC*, *UBB*, *CALR*, *CXCR4*, *JUND*, *FOS*, *PIM2*, *JUN*, *GAPDH*, and *HSP90B1* and were previously reported as upregulated in the Munshi Multiple myeloma dataset.
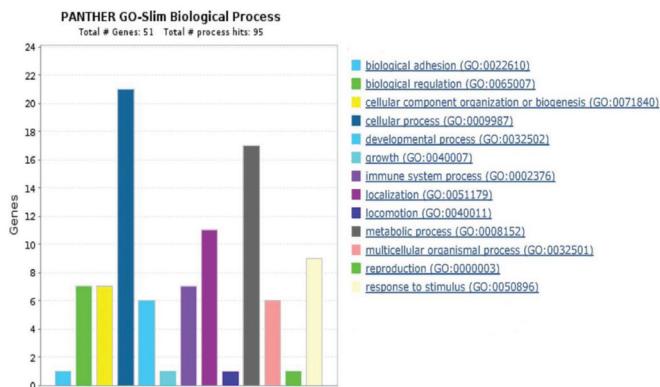

FIG. 5. Biological process analysis of the first 50 highly expressed genes according to the PANTHER program: The highest rated biological process is cellular process analyzed in bar view. It is next to the color indicator that identifies the respective GO terms and numbers according to PANTHER.
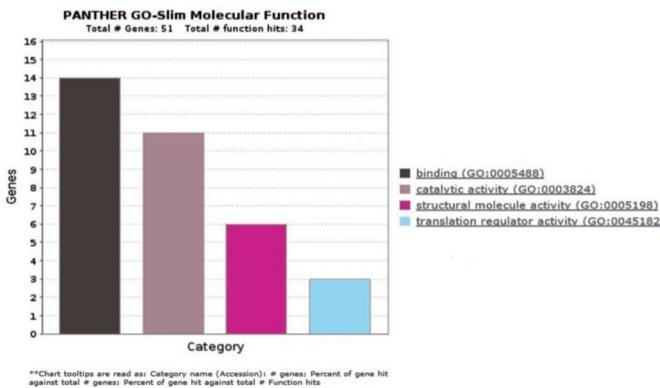

FIG. 6. Molecular function analysis of the first 50 highly expressed genes according to the PANTHER program: The highest rated molecular functions is binding analyzed in bar view. It is next to the color indicator that identifies the respective GO terms and numbers according to PANTHER.
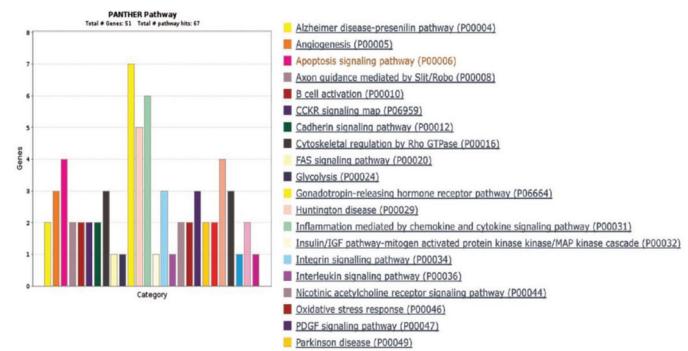
FIG. 7. Pathway analysis of the first 50 highly expressed genes according to the PANTHER program. Results of PANTHER colorful bars view show us several myeloma pathways associated with especially the B cell activation, inflammation mediated by chemokine and cytokine signaling pathway and apoptosis signaling pathway.

DISCUSSION

Decades of scientific research data backed up with array technologies and next generation sequencing technologies have shown us two important contributors to MM pathogenesis. One is the interactions between myeloma cells and the microenvironment and the other is malignant clone genetic transformation (9,10). In this study, we purified and directly sorted myeloma cells. Multicolor flow cytometry is a sensitive method to analyze plasma cell immunophenotypes and identify normal and neoplastic plasma cell populations. In our study, the surface markers of malignant B cells obtained from the literature were compared with those of the MM group with CD38(+), 138(+), CD56(+), CD19(-) B cell separation of the control group using CD38(+), 138(+), CD56(-), CD19(+) surface markers by multicolor flow cytometry (11). The

TABLE 2. Reads per kilobase of the exon model per million mapped reads values of the first 50 selected genes highly expressed in pooled in multiple myeloma cells

	Gene name	Transcript length	Transcript ID	Total transcript reads	Exons	RPKM	Chromosome	Chromosome region start	Chromosome region end
1	EEF2	3158	NM_001961.3	863	15	1256.601	NC_000019	3976054	3985461
2	HLA-B	1572	NM_005514.6	395	8	1155.429	NC_000006	31321649	31324989
3	EEF1A1	3512	NM_001402.5	819	8	1072.329	NC_000006	74225473	74230755
4	B2M	987	NM_004048.2	198	4	922.458	NC_000015	45003685	45010357
5	TXNDC5	2958	NM_030810.2	592	10	920.285	NC_000006	7881750	7911041
6	TMSB10	482	NM_021103.3	71	3	677.345	NC_000002	85132763	85133799
7	HLA-A	1549	NM_002116.6	222	8	659.022	NC_000006	29910309	29913661
8	HLA-C	1525	NM_002117.4	218	8	657.333	NC_000006	31236529	31239855
9	EEF1G	1538	NM_001404.4	217	10	648.787	NC_000011	62327073	62341460
10	ITM2C	2073	NM_030926.4	261	6	578.948	NC_000002	231729621	231743963
11	FTL	871	NM_000146.3	108	4	570.17	NC_000019	49468566	49470136
12	GNB2L1	1109	NM_006098.4	134	8	555.612	NC_000005	180663928	180670906
13	UBC	2574	NM_021009.4	295	2	527.002	NC_000012	125396192	125399577
14	FOSB	3776	NM_006732.2	409	4	498.07	NC_000019	45971253	45978437
15	GAPDH	1310	NM_002046.3	139	9	487.913	NC_000012	6643657	6647536
16	CD74	1311	NM_004355.2	137	8	480.526	NC_000005	149781209	149792330
17	JUN	3323	NM_002228.3	324	1	448.346	NC_000001	59246463	59249785
18	TXNIP	2934	NM_006472.3	271	8	424.725	NC_000001	145438462	145442635
19	RHOB	2367	NM_004040.2	216	1	419.618	NC_000002	20646835	20649201
20	FOS	2158	NM_005252.3	195	4	415.51	NC_000014	75745481	75748937
21	ACTG1	1919	NM_001614.2	170	6	407.355	NC_000017	79476999	79479827
22	CXCR4	1674	NM_003467.2	147	2	403.795	NC_000002	136871919	136875725
23	ACTB	1812	NM_001101.3	151	6	383.193	NC_000007	5566779	5570232
24	CLPTM1L	2148	NM_030782.3	177	17	378.911	NC_000005	1317999	1345002
25	VIM	2136	NM_003380.3	174	10	374.582	NC_000010	17270258	17279592
26	HBA2	605	NM_000517.4	48	3	364.825	NC_000016	222846	223709
27	HSPA8	2261	NM_006597.3	175	9	355.907	NC_000011	122928200	122932844
28	TPT1	829	NM_003295.2	64	6	354.997	NC_000013	45911304	45915297
29	DUSP1	2024	NM_004417.3	151	4	343.056	NC_000005	172195093	172198203
30	CYBA	688	NM_000101.2	51	6	340.863	NC_000016	88709697	88717457
31	PIM2	2187	NM_006875.3	161	6	338.513	NC_000023	48770459	48776413
32	HBB	626	NM_000518.4	45	3	330.55	NC_000011	5246696	5248301
33	KLF2	1655	NM_016270.2	117	3	325.077	NC_000019	16435651	16438345
34	JUND	1870	NM_005354.4	128	1	314.751	NC_000019	18390563	18392432
35	IGLL5	1059	NM_001178126.1	72	3	312.633	NC_000022	23229960	23238014
36	BTG2	2712	NM_006763.2	181	2	306.893	NC_000001	203274664	203278730
37	JUNB	1816	NM_002229.2	121	1	306.385	NC_000019	12902310	12904125
38	PPIB	1028	NM_000942.4	68	5	304.169	NC_000015	64448014	64455354
39	SDC1	3201	NM_002997.4	209	5	300.234	NC_000002	20400825	20425194

TABLE 2. Continued

|	Gene name	Transcript length	Transcript ID	Total transcript reads	Exons	RPKM	Chromosome	Chromosome region start	Chromosome region end
40	HLA-E	2662	NM_005516.5	169	8	291.929	NC_000006	30457183	30461982
41	PSAP	2822	NM_002778.2	175	14	285.154	NC_000010	73576055	73611082
42	CALR	1911	NM_004343.3	106	9	255.061	NC_000019	13049414	13055304
43	ICAM3	1780	NM_002162.3	95	7	245.416	NC_000019	10444452	10450345
44	GLTSCR2	1522	NM_015710.4	80	13	241.699	NC_000019	48248793	48260323
45	HSP90B1	2780	NM_003299.1	146	18	241.494	NC_000012	104324189	104341703
46	PTMA	1205	NM_002823.4	62	5	236.594	NC_000002	232573235	232578251
47	UBB	971	NM_018955.2	49	2	232.047	NC_000017	16284367	16286054
48	HSPA1B	2520	NM_005346.4	126	1	229.916	NC_000006	31795512	31798031
49	SIK1	4706	NM_173354.3	232	14	226.691	NC_000021	44834395	44847002
50	FAM46C	5720	NM_017709.3	271	2	217.857	NC_000001	118148604	118171011
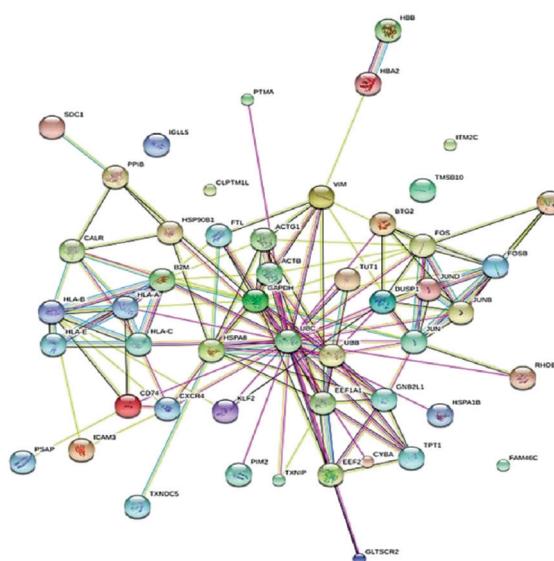
FIG. 8. Protein-protein interactions network of between the first 50 highly differentially expressed genes in myeloma cells. The network was constructed using the STRING database (http://string-db.org).

TABLE 3. Comparison of the first 50 genes which have highest reads per kilobase of the exon model per million mapped reads value in pooled multiple myeloma with pooled healthy control

	Gene name	MM pooled RPKM	Control pooled RPKM
1	EEF2	1256.601	0
2	HLA-B	1155.429	89.8001
3	EEF1A1	1072.329	101.2346
4	B2M	922.458	23.4577
5	TXNDC5	920.285	0
6	TMSB10	677.345	0
7	HLA-A	659.022	0
8	HLA-C	657.333	23.5247
9	EEF1G	648.787	19.9456
10	ITM2C	578.948	0
11	FTL	570.17	91.336
12	GNB2L1	555.612	7.4764
13	UBC	527.002	42.3771
14	FOSB	498.07	0
15	GAPDH	487.913	208.4421
16	CD74	480.526	21.0904
17	JUN	448.346	0
18	TXNIP	424.725	0
19	RHOB	419.618	0
20	FOS	415.51	0
21	ACTG1	407.355	0
22	CXCR4	403.795	0
23	ACTB	383.193	139.7349
24	CLPTM1L	378.911	0
25	VIM	374.582	4.1921
26	HBA2	364.825	301.9547
27	HSPA8	355.907	0

transcriptome patterns of the first 50 highly expressed genes in Figure 4 and in those in Figures 5-7 were analyzed, and a pathway network was constructed to better understand the relationships among them. Technologies must be developed to identify related genes that show potential to play a role in transforming normal cells into myeloma cells. GSEA MSigD identified genes were included in previously known and myelomagenesis signaling related pathways. In addition, the families of these genes were analyzed with the same program. According to the results, *JUN* was in the oncogene family; *FOSB*, *JUN*, *JUNB*, *JUND*, and *KLF* were in the transcription factor family; *PIM2* and *SIK1* were in the protein kinase family; and *CXCR4*, *CD74*, *ICAM3*, and *SDC1* were cell differentiation markers. In particular, the first 50 genes supported that the ubiquitin genes, such as *UBB*, *UBC*, *EEF2*, were related to the pathogenesis of MM. The ubiquitin cascade

TABLE 3. Continued

	Gene name	MM pooled RPKM	Control pooled RPKM
28	TPT1	354.997	94.7143
29	DUSP1	343.056	0
30	CYBA	340.863	1.6808
31	PIM2	338.513	0
32	HBB	330.55	178.691
33	KLF2	325.077	0
34	JUND	314.751	0
35	IGLL5	312.633	12.9554
36	BTG2	306.893	0
37	JUNB	306.385	0
38	PPIB	304.169	0
39	SDC1	300.234	0
40	HLA-E	291.929	0
41	PSAP	285.154	2.2344
42	CALR	255.061	0
43	ICAM3	245.416	0
44	GLTSCR2	241.699	0
45	HSP90B1	241.494	0
46	PTMA	236.594	0
47	UBB	232.047	0
48	HSPA1B	229.916	0
49	SIK1	226.691	0
50	FAM46C	217.857	0

MM: multiple myeloma; RPKM: reads per kilobase of the exon model per million mapped reads

system is a central contributor to cellular processes that regulate protein stability, trafficking, and activation (12,13). Proteosome inhibitors have been used for many years as a basic therapeutic strategy for treating MM and have been developed as antimyeloma therapy by focusing on this ubiquitin proteosome cascade (14). Losada et al. (15) reported that plitidepsin has successfully concluded a phase-III clinical trial for MM. Antitumor activity was achieved by targeting plitidepsin to *EEF1A2*. *EEF1A2* has proto-oncogenic activity, and it has been reported to be abnormally expressed in many human tumors including MM. In our study, the *EEF2*, *EEF1G*, and *EEF1A1* genes were overexpressed and may be responsible for inhibiting apoptosis and controlling unfolded protein degradation by proteasomes similar to the EEF1G gene. Prosaposin is a lysosomal protein that has pleiotropic growth factor activity. It is known to be related to the growth of breast cancer and to increase ER levels through the mitogen activated protein kinase (MAPK) pathway. In addition to gallbladder cancer, it operates as a biomarker and promotes increased degradation of ceramides, ensuring a survival advantage to cancer cells (16). Starlets et al. (17) reported that a cell surface molecule expressed on B cells binds CD74 to the macrophage migration-inhibition factor, activating CD74; thus, initiating a survival pathway. The

humanized anti-CD74 monoclonal antibody acts as a potential therapeutic agent by exhibiting cell proliferation activity in MM (18). Our findings show that CD74 is strongly expressed in myeloma cells compared to healthy cells and has a role in the oncogenic process of cell proliferation and survival. Prosaposin is a protein encoded by the *PSAP* gene that interacts with CD74 and may play a role in MM carcinogenesis (Figure 8). Despite advances in the understanding of MM pathogenesis, the molecular pathways underlying the development of MM are still unknown. Our functional and pathway enrichment analysis proposed that major histocompatibility complex class I molecules called human leukocyte antigens (HLA-A, HLA-B, HLA-C, and HLA-E) are involved. Known as antigen processing and presenting machinery (AMP), these molecules are important for cell survival, cell cycle progression, and inhibition of apoptosis. Defects in the AMP lead to immune escape and continuity by cancer. As a result, it enables malignant transformation of cells.

The enriched pathways for these upregulated genes are involved in peptide transport from the cytosol into the endoplasmic reticulum, antigen processing, peptide trimming, and assembly of the major histocompatibility complex class I loading complex (19). Leone et al. (20) compared the expression levels of calnexin, calreticulin, tapasin, and *ERp57* genes in premalignant plasma cells obtained from patients with monoclonal gammopathy of undetermined significance, those with MM, and normal plasma cells from healthy donors and showed that these levels are higher in patients with monoclonal gammopathy of undetermined significance and MM. It has been documented in cell lines from primary cells and various tumors, particularly MM, that *TAP1* and/or *TAP2* mRNA and protein levels are not detectable in small quantities. Defects in *TAP* genes play a role in the development of hematological malignancies (21). Our results included a mutated *TAP* gene (data not shown). Another related gene is calreticulin. This gene produces a calcium-binding protein that is a major component of the endoplasmic reticulum and has been shown in various cell types to be involved in regulating calcium homeostasis, as a ligand for integrins, and as a component of phagocytic synapses (22). Upregulation of the calreticulin gene is an adverse prognostic factor as the dominant pro-phagocytic signal in diverse tumors and is correlated with increased CD47 expression in cancer cells (23). The cisplatin resistance-related protein CRR9p (*CLPTM1L*) gene is overexpressed in lung cancer and knockdown of this gene prevents 95-D lung cancer cells from migrating and invading (24). Although the function of this gene is largely unknown, high expression levels of *CLPTM1L* have been observed in many cancers, and it is linked with cisplatin-induced apoptosis (25). Another study demonstrated that blocking *CLPTM1L* with interfering RNA inhibits lung tumorigenesis induced by K-RAS. That study suggested that *CLPTM1L* interacts with PI3 kinase and has a major role in *RAS*-induced *AKT* phosphorylation (26). Our results suggest that the *CLPTM1L* gene has a higher RPKM value in myeloma cells than in healthy donor cells. Cytokines and growth factors activate the phosphoinositide 3-kinase/AKT signaling cascade, creating life signals for myeloma cells by inhibiting apoptosis in MM. The RAS-MAPK pathway provides for proliferation of myeloma cells (27). The results of other studies on this gene are particularly related to PI3-K/AKT cascades, indicating

that it should be considered a plausible candidate gene. Dytfell et al. reported that increased *TXNDC5* expression in plasma cells and serum is related to a poor response to bortezomid-based therapy in patients with newly diagnosed MM and in those with relapsed MM. Understanding MM biology and identifying drug-resistance biomarkers are vital to enable the development of individualized treatments. Proteomic signature results indicate that *TXNDC5*, which is a member of the protein disulfide isomerase family, shows increased expression and is involved in protection against oxidative stress and plays a major role in bortezomib treatment (28). Using in silico tools, we identified significant overlaps between *EEF1A1*, *UBC, UBB*, *CALR*, *CXCR4, JUND*, *FOS*, *PIM2*, *JUN*, *GAPDH*, and *HSP90B1*, which were previously reported to be upregulated in MM according to the Munıshı_ MM data set (Figure 4). The Panther program revealed the results of molecular features, biological functions, and related pathways of the first 50 genes with the highest RPKM values. As we compared our findings with the results from other studies, we saw that biologic adhesion, biological processes, and metabolic processes were the same as these previous studies (Figures 5-7). Analyzing these genes using the String program may lead to further functional studies on protein-protein interactions (Figure 8). This transcriptome analysis of MM was performed for the first time in a Turkish population. As results, we determined some variations and different mRNA expression patterns in some of the previously reported genes particularly those in the ubiqutin-proteosomal pathway.

In conclusion, *EEF1G*, *ITM2C*, *FTL*, *CLPTM1L*, and *CYBA* are possible candidate genes associated with myelomagenesis.

REFERENCES

1. Hameed A, Brady JJ, Dowling P, Clynes M, O'Gorman P. Bone disease in multiple myeloma: pathophysiology and management. Cancer Growth Metastasis 2014;7:33-42.

2. Dispenzieri A, Lacy QM, Greipp RP. Wintrobe's Clinical Hematology-Volume 2 Multiple Myeloma. In: Greer JP, Foerster J, Rodgers GM, Paraskevas F, Glader B, Arber DA, et al, editors. 12th ed. USA, Philadelphia; Lippincott W & Wilkins; 2009:2372-438.

3. Kumar SK, Callander NS, Alsina M, Atanackovic D, Biermann JS, Castillo J, et al. NCCN Guidelines Insights: Multiple Myeloma, Version 3. 2018. J Natl Compr Canc Netw 2018;16:11-20.

4. Sergentanis TN, Zagouri F, Tsilimidos G, Tsagianni A, Tseliou M, Dimopoulos MA, et al. Risk Factors for Multiple Myeloma: A Systematic Review of Meta-Analyses. Clin Lymphoma Myeloma Leuk 2015;15:563-77.

5. Sawyer JR. The prognostic significance of cytogenetics and molecular profiling in multiple myeloma. Cancer Genet 2011;204:3-12.

6. Cao FF, Chen F, Hu YP, Zhang JH. Immunophenotype in multiple myeloma cells detected by multiparameter flow cytometry. Zhongguo Shi Yan Xue Ye Xue Za Zhi 2012;20:620-3.

7. Han Y, Gao S, Muegge K, Zhang W, Zhou B. Advanced Applications of RNA Sequencing and Challenges. Bioinform Biol Insights 2015;9(Suppl 1):29-46.

8. Conesa A, Madrigal P, Tarazona S, Gomez-Cabrero D, Cervera A, McPherson A, et al. A survey of best practices for RNA-seq data analysis. Genome Biol 2016;17:13.

9. Hideshima T, Mitsiades C, Tonon G, Richardson PG, Anderson KC. Understanding multiple myeloma pathogenesis in the bone marrow to identify new therapeutic targets. Nat Rev Cancer 2007;7:585-98.

10. Furukawa Y, Kikuchi J. Molecular pathogenesis of multiple myeloma. Int J Clin Oncol 2015;20:413-22.

11. Flores-Montero J, de Tute R, Paiva B, Perez JJ, Böttcher S, Wind H, et al. Immunophenotype of normal vs. myeloma plasma cells: Toward antibody panel specifications for MRD detection in multiple myeloma. Cytometry B Clin Cytom 2016;90:61-72.

12. Lub S, Maes K, Menu E, De Bruyne E, Vanderkerken K, Van Valckenborgh E. Novel strategies to target the ubiquitin proteasome system in multiple myeloma. Oncotarget 2016;7:6521-37.

13. Myung J, Kim KB, Crews CM. The ubiquitin-proteasome pathway and proteasome inhibitors. Med Res Rev 2001;21:245-73.

14. Kubiczkova L, Pour L, Sedlarikova L, Hajek R, Sevcikova S. Proteasome inhibitors - molecular basis and current perspectives in multiple myeloma. J Cell Mol Med 2014;18:947-61.

15. Losada A, Muñoz-Alonso MJ, García C, Sánchez-Murcia PA, Martínez-Leal JF, Domínguez JM, et al. Translation Elongation Factor eEF1A2 is a Novel Anticancer Target for the Marine Natural Product Plitidepsin. Sci Rep 2016;6:35100.

16. Sahasrabuddhe NA, Barbhuiya MA, Bhunia S, Subbannayya T, Gowda H, Advani J, et al. Identification of prosaposin and transgelin as potential biomarkers for gallbladder cancer using quantitative proteomics. Biochem Biophys Res Commun 2014;446:863-9.

17. Starlets D, Gore Y, Binsky I, Haran M, Harpaz N, Shvidel L, et al. Cell-surface CD74 initiates a signaling cascade leading to cell proliferation and survival. Blood 2006;107:4807-16.

18. Stein R, Qu Z, Cardillo TM, Chen S, Rosario A, Horak ID, et al. Antiproliferative activity of a humanized anti-CD74 monoclonal antibody, hLL1, on B-cell malignancies. Blood 2004;104:3705-11.

19. Lecker SH, Goldberg AL, Mitch WE. Protein degradation by the ubiquitin-proteasome pathway in normal and disease states. J Am Soc Nephrol 2006;17:1807-19.

20. Leone P, Shin EC, Perosa F, Vacca A, Dammacco F, Racanelli V. MHC class I antigen processing and presenting machinery: organization, function, and defects in tumor cells. J Natl Cancer Inst 2013;105:1172-87.

21. Ozbas-Gerceker F, Bozman N, Gezici S, Pehlivan M, Yilmaz M, Pehlivan S, et al. Association of TAP1 and TAP2 gene polymorphisms with hematological malignancies. Asian Pac J Cancer Prev 2013;14:5213-7.

22. Zhou P, Teruya-Feldstein J, Lu P, Fleisher M, Olshen A, Comenzo RL. Calreticulin expression in the clonal plasma cells of patients with systemic light-chain (AL-) amyloidosis is associated with response to high-dose melphalan. Blood 2008;111:549-57.

23. Chao MP, Jaiswal S, Weissman-Tsukamoto R, Alizadeh AA, Gentles AJ, Volkmer J, et al. Calreticulin is the dominant pro-phagocytic signal on multiple human cancers and is counterbalanced by CD47. Sci Transl Med 2010;2:63ra94.

24. Ni Z, Chen Q, Lai Y, Wang Z, Sun L, Luo X, et al. Prognostic significance of CLPTM1L expression and its effects on migration and invasion of human lung cancer cells. Cancer Biomark 2016;16:445-52.

25. Yin J, Li Y, Yin M, Sun J, Liu L, Qin Q, et al. TERT-CLPTM1L polymorphism rs401681 contributes to cancers risk: evidence from a meta-analysis based on 29 publications. PLoS One 2012;7:50650.

26. James MA, Vikis HG, Tate E, Rymaszewski AL, You M. CRR9/CLPTM1L regulates cell survival signaling and is required for Ras transformation and lung tumorigenesis. Cancer Res 2014;74:1116-27.

27. Steinbrunn T, Stühmer T, Sayehli C, Chatterjee M, Einsele H, Bargou RC. Combined targeting of MEK/MAPK and PI3K/Akt signalling in multiple myeloma. Br J Haematol 2012;159:430-40.

28. Dytfeld D, Luczak M, Wrobel T, Usnarska-Zubkiewicz L, Brzezniakiewicz K, Jamroziak K, et al. Comparative proteomic profiling of refractory/relapsed multiple myeloma reveals biomarkers involved in resistance to bortezomib-based therapy. Oncotarget 2016;7:56726-36.